arXiv:1609.06292v1 [cond-mat.mes-hall] 20 Sep 2016

Solitons in one-dimensional lattices with a flat band

Dario Bercioux,[1,2,*] Omjyoti Dutta,[1] and Enrique Rico[2,3]

[1] *Donostia International Physics Center (DIPC), Manuel de Lardizbal 4, E-20018 San Sebastián, Spain*

[2] *IKERBASQUE, Basque Foundation for Science, Maria Diaz de Haro 3, 48013 Bilbao, Spain*

[3] *Department of Physical Chemistry, University of the Basque Country UPV/EHU, Apartado 644, E-48080 Bilbao, Spain*

We investigate the spectral properties of a quasi-one-dimensional lattices in two possible dimerization configurations. Both configurations are characterized by the same lattice topology and the same spectra containing a flat band at zero energy. We find that, one of the dimerized configuration has similar symmetry to an one-dimensional chain proposed by Su-Schrieffer-Heeger for studying solitons in conjugated polymers. Whereas, the other dimerized configuration only shows non-trivial topological properties in the presence of chiral-symmetry breaking adiabatic pumping.

PACS numbers:

I. INTRODUCTION

Lattice systems with flat bands have been of great interest in the past years. On one side, research was devoted in finding possible correlated states leading to fractional quantum Hall states without applied magnetic field [1–3]. In parallel, there has been a research activity devoted to investigate the presence of flat bands in two-dimensional (2D) lattices as the $\mathcal{T}_3$ [4–6] or the Lieb [7] lattice for possible application to cold atoms in optical lattices [8–11], photonic crystals [12, 13] and exciton polaritons [14, 15]. These 2D systems [16] — both characterized by a pseudo-spin 1 — present peculiar transport properties, the so called *super Klein tunneling*, where the tunneling probability for a particle going through a potential barrier is unitary independently of the incidence angle and barrier length [17–20]. This scattering mechanisms has also potential applications in the framework of photonic crystals [21] and quantum optics [22].

In the past few years, the attention has moved to research of three-dimensional (3D) structure that presents a Dirac cone with a flat band in the middle of the cone, this corresponds to a 3D representation of pseudo-spin 1. In a first proposal based on HgCdTe quantum well, this triple degeneracy point has been achieved by playing with doping level of Cd in the quantum well heterostructure. This triple degeneracy point has also been observed experimentally [23–25]. The second one is a theoretical proposal for a crystal structure with an intrinsically protected triple degeneracy point [26].

In the present work we investigate topological property of a dimerized one-dimensional chain containing flat bands. Our prototype model is the one-dimensional dimer chain, or one-dimensional Su-Schrieffer-Heeger (SSH) model, originally introduced to describe solitonic effects in polymers [27–29]. Such a dimer chain supports edge states when it is in the topologically non-trivial phase [30]. The SSH model shows topological non trivial properties also in the presence of Coulomb interaction [31].

A quasi-one-dimensional lattice with a flat band can be obtained by considering a bipartite lattice with a unit cell containing three lattice sites with unequal connectivity [Fig. 1(a)] — we name this lattice in the following diamond chain [32]. In this system, there is a lattice site — called Hub or H in the following — that has four next-neighbor and two Rim sites, A and B, respectively. These have only two next neighbor that are always hub sites; it is not possible in this system to move directly from A to B, this is allowed only via an hub site. This bipartite structure with inequivalent sites in the unit cell is at the origin of the flat band [4, 16]. The interest in investigating this diamond lattice roots in the possibility to implement a lattice dimerization in two different ways. We will illustrate, via fundamental symmetry arguments, that the two dimerization configurations lead to opposite topological properties.

The diamond chain is also interesting because it has been proposed recently an implementation with optical lattices by Hyrkas *et al.* [33] This is not the only possibility to implement a lattice chain with a flat band, other lattices with flat bands are present in the literature [34, 35]. Several pioneering works already addressed the role of a flat band in photonic systems [13, 36, 37] and cold-atom gases [9, 10] where the key role played by geometric frustration was highlighted [38] and evidenced characteristic features such as the absence of wave packet diffraction in a flat band was studied [13].

This article is organized in the following way: in Sec. II we present the diamond chain in the two possible dimerization configuration we have disclosed. In Sec. III we present the topological properties of these two lattice configurations. We conclude the manuscript with a discussion of our finding and suggestions for possible experimental implementations.

*Electronic address: dario.bercioux@dipc.org

II. MODELS AND FORMALISM

We consider a prototypical quasi-one dimensional lattice with a flat band: a diamond chain containing three distinct sites in the unit cell [see Fig. 1(a)]. In Fig. 1(a) we denote the three sub-lattices as H (or Hub with coordination number four), Rim A and B (or simply A and B), both with coordination number two. The drawing with a square path as in Fig. 1(a) is ideal when considering the effects of an external magnetic field [32, 39, 40] or of a spin-orbit coupling [32, 40]. If external fields are absent we can consider a stretch version as the one shown in Fig. 1(b) that facilitated the identification of lattice symmetries. In case of equal hopping amplitudes, $t_i \equiv t\ \forall i$, each axes perpendicular to the chain and passing though a site H is an inversion axes. In the following we will focus on the possible set of hopping amplitudes that lead to a dimerization of the diamond chain, in the same spirit as that of SSH model [27, 28]. Specifically, we have isolated two possible choice for the hopping parameters, the first one — named in the following *lattice I* — is characterized by $t_1 = t_4 = t$ and $t_2 = t_3 = t'$; the second one — named *lattice II* — is characterized by $t_1 = t_3 = t$ and $t_2 = t_4 = t'$. The two lattices are shown in Fig. 1(c) and 1(d), respectively. From the figure, we immediately observe that contrary to the SSH model, for both dimerization configurations we can not find an inversion axes. These dimerization configurations are equivalent to consider two SSH chains-sharing a common lattice site — the H in the specific of our models. The main difference is that in the case of lattice I the two dimerized chains are parallel, whereas in the case of lattice II, the dimerization of the lower chain is shifted of a unit cell with respect to the upper one. The results we are going to present are strongly affected by the presence of the common lattice site that is acting as an effective boundary condition.

A. Spectrum and Symmetries

1. Lattice I

For this lattice, we first write a tight-binding Hamiltonian as,

$$\mathcal{H}_{\rm I} = \sum_n t\ h_n^\dagger(a_n + b_n) + t'\ (a_n^\dagger + b_n^\dagger)h_{n+1} + \text{h.c.}\,, \quad (1)$$

where n is the index for unit cell. The sub-lattice annihilation operators are denote by $h_n^{(\dagger)}$, $a_n^{(\dagger)}$, $b_n^{(\dagger)}$ for a particle on the sites H, A and B of unit cell n [Fig. 1(c)], respectively. Assuming translational invariance, we can write down the Hamiltonian (1) in the reciprocal space as:

$$\begin{aligned}[\mathcal{H}_I]_k &= h_x(k)\Sigma_x^{\rm I} + h_y(k)\Sigma_y^{\rm I},\\ h_1(k) &= \sqrt{2}(t + t'\cos kL); h_2 = \sqrt{2}t'\sin kL, \end{aligned} \quad (2)$$

where,

$$\Sigma_x^{\rm I} = \frac{1}{\sqrt{2}}\begin{pmatrix}0&1&0\\1&0&1\\0&1&0\end{pmatrix} \qquad \Sigma_y^{\rm I} = \frac{1}{\sqrt{2}}\begin{pmatrix}0&-\mathrm{i}&0\\\mathrm{i}&0&\mathrm{i}\\0&-\mathrm{i}&0\end{pmatrix} \quad (3a)$$

$$\Sigma_z^{\rm I} = \frac{1}{2}\begin{pmatrix}1&0&1\\0&-2&0\\1&0&1\end{pmatrix} \qquad \mathcal{I} = \frac{1}{2}\begin{pmatrix}1&0&1\\0&2&0\\1&0&1\end{pmatrix}. \quad (3b)$$

Here we have introduced additional matrices $\Sigma_z^{\rm I}, \mathcal{I}$ so that $\{\mathcal{I}, \Sigma_x^{\rm I}, \Sigma_y^{\rm I}, \Sigma_z^{\rm I}\}$ form an orthogonal basis with SU(2) Lie algebra: $[\Sigma_i^{\rm I}, \Sigma_j^{\rm I}] = 2\mathrm{i}\epsilon_{ijk}\Sigma_k^{\rm I}$ where ϵ_{ijk} is Levi-Civita tensor with $i, j, k \in \{x, y, z\}$ and $[\cdot,\cdot]$ is the commutator. Note that these four matrix operators form a closed subgroup of SU(3). As a result, the Hamiltonian Eq. (2) is equivalent to the SSH Hamiltonian [27, 28]. Subsequently, $\Sigma_z^{\rm I}$ (equivalent of σ_z operator for SSH model) acts as a chiral operator: $\Sigma_z^{\rm I}[\mathcal{H}_{\rm I}]_k\Sigma_z^{\rm I} = -[\mathcal{H}_{\rm I}]_k$. As a result, following SSH model we can expect a topological phase transition as one changes the ratio t/t'.

The Hamiltonian (2) has the following spectrum,

$$\mathcal{E}_0^{\rm I} = 0 \quad (4a)$$

$$\mathcal{E}_\pm^{\rm I} = \pm\sqrt{2}\sqrt{t^2 + (t')^2 + 2t't\cos(kL)} \quad (4b)$$

and eigenstates,

$$|v_0^{\rm I}(k)\rangle = \frac{1}{\sqrt{2}}(-1, 0, 1) \quad (5a)$$

$$|v_\pm^{\rm I}(k)\rangle = \frac{1}{\sqrt{2}}\left(\frac{\mathrm{e}^{\mathrm{i}\phi(k)}}{\sqrt{2}}, \pm 1, \frac{\mathrm{e}^{\mathrm{i}\phi(k)}}{\sqrt{2}}\right). \quad (5b)$$

where $\phi(k) = -\arctan\left[\frac{\sin(kL)}{t/t'+\cos(kL)}\right]$. The spectrum consists of two particle-hole dispersive bands with an absolute maximum and minimum at $k = 0$ and relative maximum and minimum at band boundary $k = \pi/L$. The gap at the band boundary is directly proportional to the difference of the two hopping amplitude $m = (t - t')$, and is zero in absence of dimerization $m = 0$. In addition to these two bands, from Eq. (4a) we notice the presence of a flat band at zero energy. This is characterized by an eigenstate (5a) that have amplitudes finite and opposite only of the A and B sites, while it is exactly equal to zero on the H sites.

2. Lattice II

For the lattice II, we redefine the sub-lattice of a unit cell by H, site A on right neighbor of H and site B on the left neighbor of H [Fig. 1(d)]. Such redefinition helps us to compare the resulting Hamiltonian from that of lattice I. The Hamiltonian for lattice II then reads:

$$\mathcal{H}_{\rm II} = \sum_n t\ (h_n^\dagger a_n + h_n^\dagger b_n) + t'\ (h_n^\dagger a_{n-1} + h_n^\dagger b_{n+1}) + \text{h.c.}\,. \quad (6)$$

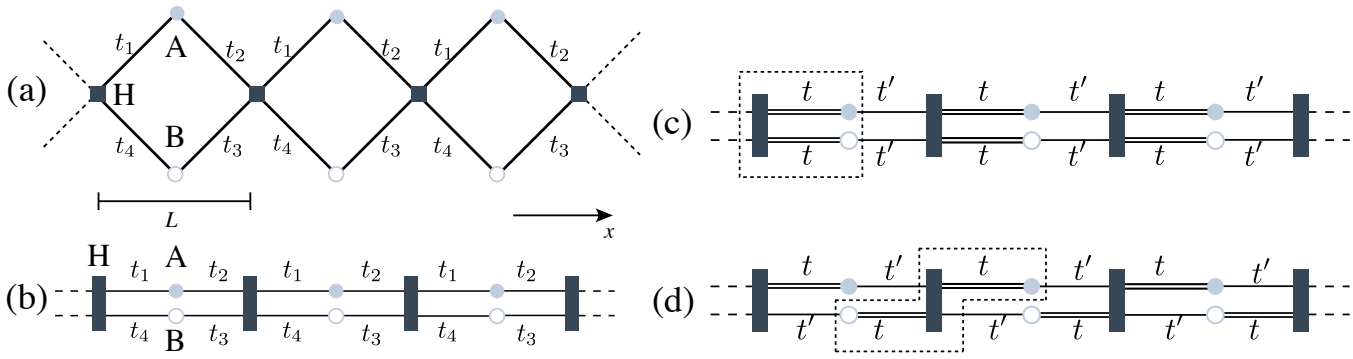

Figure 1: Sketch of the diamond chain (a); same lattice but stretch in a quasi-one-dimension form (b); dimerized form of the diamond chain: lattice I (c); lattice II (d), the dashed boxes show the two unit cells. The two lattices differs for the position of the double bonds, in lattice I these are parallel whereas in lattice II they are shifted of a lattice site.

This tight-binding Hamiltonian in the reciprocal space reads:

$$[\mathcal{H}_{\rm II}]_k \;=\; h_x(k)\Sigma_x^{\rm II} + h_y(k)\Sigma_y^{\rm II}, \tag{7}$$

where,

$$\Sigma_1^{\rm II} = \frac{1}{\sqrt{2}}\begin{pmatrix} 0 & 1 & 0 \\ 1 & 0 & 1 \\ 0 & 1 & 0 \end{pmatrix} \qquad \Sigma_y^{\rm II} = \frac{1}{\sqrt{2}}\begin{pmatrix} 0 & \mathrm{i} & 0 \\ -\mathrm{i} & 0 & \mathrm{i} \\ 0 & -\mathrm{i} & 0 \end{pmatrix}. \tag{8}$$

Comparing Eq.(3a) and (8), we immediately recognize that

$$\Sigma_x^{\rm I} = \Sigma_x^{\rm II} \tag{9a}$$
$$\Sigma_y^{\rm I} \neq \Sigma_y^{\rm II}. \tag{9b}$$

The last inequality has an important impact as one cannot find an equivalent basis with SU(2) Lie algebra using $\Sigma_{x,y}^{\rm II}$ and their commutator. As a result, the lattice II is not equivalent to a SSH model and will not show any topological phase transition when tuning t/t'. To look for possible topological transitions in this phase, we first identify the sub-lattice symmetry operator,

$$\Gamma = \begin{pmatrix} 1 & 0 & 0 \\ 0 & -1 & 0 \\ 0 & 0 & 1 \end{pmatrix}. \tag{10}$$

that anti-commutes with $[\mathcal{H}_{\rm II}]_k$: $\Gamma^\dagger[\mathcal{H}_{\rm II}]_k\Gamma = -[\mathcal{H}_{\rm II}]_k$. One way to induce topological phase transition in this system is by breaking this sub-lattice symmetry, as we will show later.

The spectrum of lattice II is completely identical the one of lattice I:

$$\mathcal{E}_0^{\rm II} = 0 \tag{11a}$$
$$\mathcal{E}_\pm^{\rm II} = \pm\sqrt{2}\sqrt{t^2 + (t')^2 + 2t't\cos(kL)} \tag{11b}$$

Whereas the eigenstates differs from that of lattice I,

$$|v_0^{\rm II}(k)\rangle = \frac{1}{\sqrt{2}}\left(-\mathrm{e}^{\mathrm{i}\phi(k)}, 0, \mathrm{e}^{-\mathrm{i}\phi(k)}\right) \tag{12a}$$
$$|v_\pm^{\rm II}(k)\rangle = \frac{1}{\sqrt{2}}\left(\frac{1}{\sqrt{2}}\mathrm{e}^{\mathrm{i}\phi(k)}, \pm 1, \frac{1}{\sqrt{2}}\mathrm{e}^{-\mathrm{i}\phi(k)}\right). \tag{12b}$$

Note that the phase factors enter always with opposite sign on the A and B components. As for lattice I, the flat band eigenstate (12a) is characterized by amplitudes finite and opposite on A and B while it is zero on H. This is a consequence on the bipartite nature of the two lattices [16].

III. TOPOLOGICAL PROPERTIES

In this section we investigate the topological properties of lattice I and II. At first, we look into the fully dimerized case: $t = 1$ and $t' = 0$. As in the SSH model [27], we observe the formation of isolated dimers is a signature of topological properties. The schematic of the two lattices

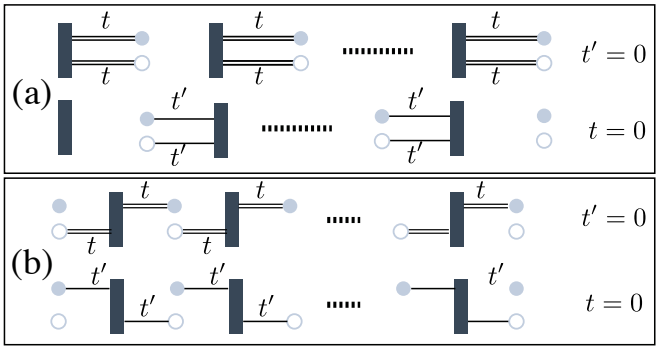

Figure 2: Fully dimerized version of lattice I (a) and lattice II (b). In the case of lattice I, the two phases cannot be mapped one into the other by any symmetry operation, in the case of lattice II the two phases are equivalent via a C_2 rotation.

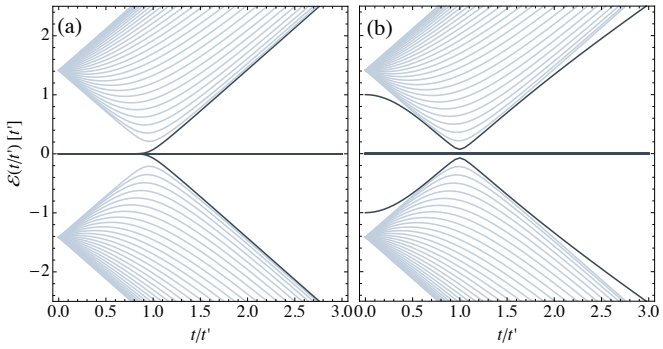

Figure 3: Energy spectrum for: (a) lattice I and (b) lattice II, as function of t/t' for a finite chain with $N = 30$ unit cells.

are shown in two panels of Fig. 2. We immediately see that only for the lattice I, we obtain a dimerization similar to the one of the SSH model [30]. Whereas for the lattice II, the two fully dimerized cases coincide up to a C_2 rotation.

Furthermore, to identify topological phase transition, we have evaluated the Zak phase for the lowest band, which is nothing but the integration of Berry connection over the first Brillouin zone [30, 41]

$$\mathcal{Z}^a = \mathrm{i}\oint dk\,\langle v_-^a(k)|\,\partial_k\,|v_-^a(k)\rangle\,,\quad a\in\{\mathrm{I,II}\} \tag{13}$$

where the $|v_-^{\mathrm{I,II}}(k)\rangle$ are defined in Eqs. (5) and (12). As expected from our discussion on structure of the Hamiltonians in Eq. (2) and (7), we find that

$$\mathcal{Z}^{\mathrm{I}} = \begin{cases} 0 & t > t' \\ \pi & t < t' \end{cases} \tag{14a}$$

$$\mathcal{Z}^{\mathrm{II}} = 0;\quad \forall t, t'. \tag{14b}$$

This shows that by tuning t/t' for lattice I across the metallic point at $t = t'$, the topological property of lattice I changes. Whereas, there is no topological transition across the metallic point for lattice II.

Due to bulk-edge correspondence, the topological properties of lattice I and II can also be seen in appearances of zero energy edge state. This is clearly seen in the spectrum for a finite chain in Fig. 3. For lattice I, as one tunes from $t/t' > 1$ to $t/t' < 1$, Fig. 3(a) shows that two energy eigenstate from the continuous band transforms to two additional zero energy states. We infer that the wave-functions for these two additional zero energy states corresponds to the left and right edge states of fully dimerized case in Fig. 2(a). This also shows the equivalence between lattice I and the SSH model. On the other hand, from spectrum of lattice II in Fig. 3(b), we see that there is no crossing as one tunes through the metallic point – consistent with no topological phase transition.

A. Topological charge pumping

Topological charge pumping refers to quantized current created due to periodic driving of a set of Hamiltonian parameters [42]. Within the adiabatic limit, such pumping are characterized by appearance of edge states in the spectrum. Such pumping is related to two-dimensional topological insulator and are characterized by Chern numbers. According to Ref.[43], for insulators without time-reversal symmetry, a topologically non-trivial pump has a broken sub-lattice symmetry. Moreover, due to adiabaticity condition, at each instance of pumping cycle, the spectrum should be gapped. As a result we choose the following time-dependent Hamiltonian:

$$[\mathcal{H}_a]_k = \sum_{i\in\{x,y\}} h_i(k,T)\Sigma_i^a + \Delta\sin(T)\tau,\quad a\in\{\mathrm{I,II}\} \tag{15}$$

where,

$$\tau = \begin{pmatrix} 1 & 0 & 0 \\ 0 & -1 & 0 \\ 0 & 0 & 0 \end{pmatrix}. \tag{16}$$

In Eq. (15) we have introduced time dependent hopping parameters: $t = 1 + m\cos(T), t' = 1 - m\cos(T)$, where T is the normalized time and m is the amplitude of tunneling dimerization. It is clear that presence of τ breaks the chiral/sub-lattice symmetry for lattice I/II. For lattice I,the pumping induces a closed path around the metallic point and acquires a Berry phase due to topological property of time-independent Hamiltonian. As a result, over a cycle, total pumped charge is given by the Chern number of the occupying band (in present case, the lowest

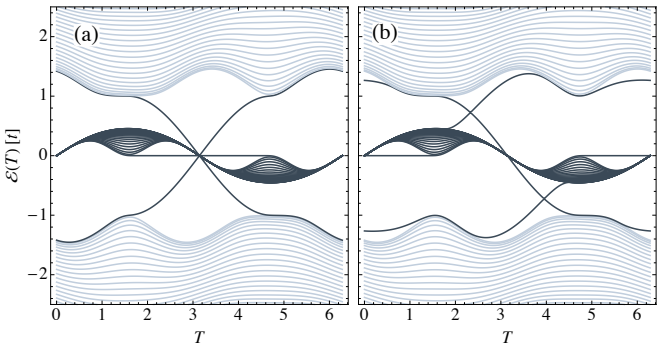

Figure 4: In the adiabatic limit, the instantaneous spectrum at time T for: (a) lattice I and (b) lattice II, corresponding to the Hamiltonian in Eq.(15). The dark lines denotes the edge states. In both panels we have considered finite chains with $N = 30$ unit cells.

band),

$$C_-^a = -\frac{i}{2\pi}\int_0^{2\pi} dT \int_{-\frac{\pi}{L}}^{\frac{\pi}{L}} dk \left[\delta_k \langle v_-^a(k,T)|\, \delta_T\, |v_-^a(k,T)\rangle - \delta_T \langle v_-^a(k,T)|\, \delta_k\, |v_-^a(k,T)\rangle\right], \quad (17)$$

where $|v_-^a(k,T)\rangle$ is the instantaneous wave-function of the lower band for Hamiltonian (15). We find that for the present model, charge pumping is same as the SSH model, $C_-^{\rm I} = 1$. This is also seen in the instantaneous spectrum of lattice I when considering a finite length chain [Fig. 4(a)]. The edge states are denoted by dark lines and at $T = \pi$, where the chiral symmetry is restored, the edge states have zero energy. On the other hand, without pumping, lattice II is topologically trivial insulator. But as seen in Fig. 4(b), in the presence of sub-lattice symmetry breaking pumping, edge state arises within a cycle both in the lower and higher band gap. As a result, lattice II has also a topological charge of $C_-^{\rm II} = 1$ and quantized current can be observed. Such topological insulators belong to class A of the classification for adiabatic topological insulators in Ref. [43].

B. Continuum limit

We can analyse the formation of edge states also studying the zero energy solution of the continuum limit of Hamiltonians (2) and (7). For both systems the spectra are insensitive to the relative difference of the two hopping amplitudes $m = t - t'$. We can look at an overall mirror symmetry $\Sigma_x^{\rm I}$ that exchange the lattice site H with A or B. The expectation value of this symmetry operator at the band boundary is:

$$\langle \Sigma_x^{\rm I}\rangle_{k=\frac{\pi}{L}} = \text{sign}[m].$$

Therefore, a a change of sign of m results is a change of parity of the dispersive bands. This change of parity, equivalent to a *band inversion*, is the signature of the existence of zero energy states.

We introduce in the following, for simplicity, a normalized dimerization parameter m in the tunneling as, $t = 1 + m/2$, $t' = 1 - m/2$. We expand then the Hamiltonians at the band boundary $k = \frac{\pi}{L} + \delta q$. As a result, from (2), (7) we get

$$h_x(k) \approx \sqrt{2} m$$
$$h_y(k) \approx -\sqrt{2}\delta q\,.$$

Next, we assume that the dimerization changes as a function of position along chain axis x with $m(x) < 0$, $x > 0$; $m(x) > 0$, $x < 0$, *i.e.*, we places a domain wall at $x = 0$. Consequently we use the transformation: $\delta q \to -\mathrm{i}\frac{d}{dx}$ to express the Hamiltonian as,

$$\mathcal{H}_a = \sqrt{2} m \Sigma_x^a + \sqrt{2}\left(\mathrm{i}\frac{d}{dx}\right)\Sigma_y^a; \quad a \in \{\mathrm{I}, \mathrm{II}\}. \quad (18)$$

We then look for the zero energy solution, $\mathcal{H}_a \Psi_a(x) = 0$ with wave-function $\Psi_a(x) = [\psi_{\rm A}^a(x), \psi_{\rm H}^a(x), \psi_{\rm B}^a(x)]^{\rm T}$, where A, H, B denote the sub-lattices in a unit cell and T is the transpose operator. Moreover, we impose the constraint of localized solution: $\Psi_a(x \to \pm\infty) \to 0$. For lattice I, Eq. (18) we obtain a set Dirac-like equation:

$$\left(\frac{d}{dx} + m(x)\right)\psi_{\rm H}^{\rm I}(x) = 0 \quad (19a)$$
$$\left(\frac{d}{dx} - m(x)\right)(\psi_{\rm A}^{\rm I}(x) + \psi_{\rm B}^{\rm I}(x)) = 0. \quad (19b)$$

For our choice of dimerization we can find a Jackiw-Rebbi solitonic solution [44] of Eqs. (19) that reads:

$$\Psi_{\rm I}(x) = \begin{pmatrix}\psi_{\rm A}\\ 0\\ \psi_{\rm B}\end{pmatrix} \exp[\int_0^x m(x')dx']$$

On the other hand, for lattice II, the Dirac-like Eq. (18) for the localized solitons are given by,

$$\left(\frac{d}{dx} - m(x)\right)\psi_{\rm H}^{\rm II}(x) = 0 \quad (20a)$$
$$\left(\frac{d}{dx} + m(x)\right)\psi_{\rm H}^{\rm II}(x) = 0 \quad (20b)$$
$$\left(\frac{d}{dx} - m(x)\right)\psi_{\rm A}^{\rm II}(x) + \left(\frac{d}{dx} + m(x)\right)\psi_{\rm B}^{\rm II}(x) = 0. \quad (20c)$$

We clearly see that, for any shape of dimerization parameter $m(x)$, the first two equations in (20) and are incompatible except for $\psi_{\rm H}^{\rm II}(x) = 0$. Moreover, for our choice of dimerization, the solution of Eq. (**??**) is $\psi_{\rm A}^{\rm II}(x) = \psi_{\rm A}\exp[\int_0^x m(x')dx']; \psi_{\rm B}^{\rm II}(x) = 0$. In-spite of presence of this localized solution in lattice II, one can show that this zero energy solution is not protected. For example, by introducing coupling between A sites and B sites, this localized solution becomes unstable.

IV. DISCUSSION, CONCLUSIONS AND OUTLOOK

In this manuscript, we have analyzed the spectral and the topological properties of two dimerized lattices presenting the same spectra, however, the two different dimerization configurations manifest in different eigenstates leading to different topological properties. The deepest mathematical difference between lattice I and II is that for the former, the relative Hamiltonian can be expressed in terms of *spin*-operators forming a SU(2) subgroup of SU(3). The other dimerization configuration do not allow to identify a similar sub-group. On the other side, when considering the continuum limit for the case of lattice II, we have show the presence of a zero energy

solitonic solution; this seems to be an accidental solution that can be destroyed by any small perturbation applied to the system. By identify the spin operator Σ_z^{I} as chiral symmetry [30], we have that lattice I is in class AIII accordingly to standard Hamiltonian classification whereas lattice II is in class A [45]. Already from this conventional classification scheme we can evince the topological nature of lattice I and the trivial nature of lattice II.

Another interesting aspect is the comparison with the case of the parallel double SSH model [46]. In this case, the authors were able to find solitonic solution also when the two parallel chains presents a dimerization out of phase, as for the case of lattice II. This routes to the different boundary conditions; in fact, in Ref. [46] the two chains are coupled by a standard hopping term, whereas in the dimerized diamond chain, the two lattices are sharing a lattice site — the Hub site. Effectively, this can be thought as a boundary condition for the overall wave function of the system.

An implementation of the diamond chain with optical lattices has been proposed in Ref. [33], however this scheme foresees homogeneous hopping amplitudes. Thus, a scheme for implementing the two dimerization configurations we have proposed needs to exploits some other property, *e.g.*, an internal degree of freedom of the cold atoms loaded in the optical lattice. At the date, the quantum simulation of topological insulators has been achieved in several platforms from photonic systems to atomic physics setup. A major issue is to explicitly reveal the topological properties of the system, *i.e.*, by measuring the topological invariants[10, 47–50] or observing their edge physics[51]. In this respect, we will show in a forthcoming publication how to reach this goal within circuit QED architectures.

Acknowledgments

We acknowledge useful discussions with A. Altland, A. Bernevig, P. Brouwer, R. Resta and I. Souza. The work of DB is supported by Spanish Ministerio de Economía y Competitividad (MINECO) through the project FIS2014-55987-P and by the Transnational Common Laboratory *QuantumChemPhys: Theoretical Chemistry and Physics at the Quantum Scale*. The work of ER is supported by a UPV/EHU grant EHUA15/17 and by Spanish Ministerio de Economía y Competitividad through the project MINECO/FEDER FIS2015-69983-P.

[1] E. Tang, J.-W. Mei, and X.-G. Wen, Phys. Rev. Lett. **106**, 236802 (2011).
[2] T. Neupert, L. Santos, C. Chamon, and C. Mudry, Phys. Rev. Lett. **106**, 236804 (2011).
[3] K. Sun, Z. Gu, H. Katsura, and S. das Sarma, Phys. Rev. Lett. **106**, 236803 (2011).
[4] D. Bercioux, D. F. Urban, H. Grabert, and W. Haeusler, Phys. Rev. A **80**, 063603 (2009).
[5] D. Bercioux, N. Goldman, and D. F. Urban, Phys. Rev. A **83**, 023609 (2011).
[6] O. Dutta, A. Przysiezna, and J. Zakrzewski, Sci. Rep. **5** (2015), 10.1038/srep11060.
[7] N. Goldman, D. Urban, and D. Bercioux, Phys. Rev. A **83** (2011), 10.1103/PhysRevA.83.063601.
[8] G. Möller and N. R. Cooper, Phys. Rev. Lett. **108**, 045306 (2012).
[9] G.-B. Jo, J. Guzman, C. K. Thomas, P. Hosur, A. Vishwanath, and D. M. Stamper-Kurn, Phys. Rev. Lett. **108**, 045305 (2012).
[10] M. Aidelsburger, M. Lohse, C. Schweizer, M. Atala, J. Barreiro, S. Nascimbene, N. Cooper, I. Bloch, and N. Goldman, Nat. Phys. **11**, 162 (2015).
[11] O. Dutta, M. Gajda, P. Hauke, M. Lewenstein, D. Lühmann, B. A. Malomed, T. Sowiński, and J. Zakrzewski, Rep. Prog. Phys. **78**, 066001 (2015).
[12] R. A. Vicencio, C. Cantillano, L. Morales-Inostroza, B. Real, C. Mejía-Cortés, S. Weimann, A. Szameit, and M. I. Molina, Phys. Rev. Lett. **114**, 245503 (2015).
[13] S. Mukherjee, A. Spracklen, D. Choudhury, N. Goldman, P. Öhberg, E. Andersson, and R. R. Thomson, Phys. Rev. Lett. **114**, 245504 (2015).
[14] S. Schmidt, Phys. Scripta **91**, 1 (2016).
[15] F. Baboux, L. Ge, T. Jacqmin, M. Biondi, E. Galopin, A. Lemaître, L. Le Gratiet, I. Sagnes, S. Schmidt, H. E. Türeci, A. Amo, and J. Bloch, Phys. Rev. Lett. **116**, 066402 (2016).
[16] Z. Lin and Z. Liu, J. Chem. Phys **143**, 214109 (2015).
[17] R. Shen, L. B. Shao, B. Wang, and D. Y. Xing, Phys. Rev. B **81**, 041410 (2010).
[18] D. F. Urban, D. Bercioux, M. Wimmer, and W. Häusler, Phys. Rev. B **84**, 115136 (2011).
[19] B. Dóra, J. Kailasvuori, and R. Moessner, Phys. Rev. B **84**, 195422 (2011).
[20] Z. Lan, N. Goldman, A. Bermudez, W. Lu, and P. Öhberg, Phys. Rev. B **84**, 165115 (2011).
[21] A. Fang, Z. Q. Zhang, S. G. Louie, and C. T. Chan, Phys. Rev. B **93**, 035422 (2016).
[22] D. Leykam and A. S. Desyatnikov, Adv. Phys.: X **1**, 101 (2016).
[23] M. Orlita, D. M. Basko, M. S. Zholudev, F. Teppe, W. Knap, V. I. Gavrilenko, N. N. Mikhailov, S. A. Dvoretskii, P. Neugebauer, C. Faugeras, A.-L. Barra, G. Martinez, and M. Potemski, Nat. Phys. **10**, 233 (2014).
[24] J. D. Malcolm and E. J. Nicol, Phys. Rev. B **92**, 035118 (2015).
[25] F. Teppe, M. Marcinkiewicz, S. Krishtopenko, S. Ruffenach, C. Consejo, A. Kadykov, W. Desrat, D. But, W. Knap, J. Ludwig, S. Moon, D. Smirnov, M. Orlita, Z. Jiang, S. Morozov, V. Gavrilenko, N. Mikhailov, and S. Dvoretskii, arXiv.org (2016), 1602.05999 .
[26] B. Bradlyn, J. Cano, Z. Wang, M. G. Vergniory, C. Felser, R. J. Cava, and B. A. Bernevig, Science **355**, 5037 (2016).

[27] W. P. Su, J. R. Schrieffer, and A. J. Heeger, Phys. Rev. Lett. **42**, 1698 (1979).

[28] W. P. Su, J. R. Schrieffer, and A. J. Heeger, Phys. Rev. B **22**, 2099 (1980).

[29] A. J. Heeger, S. Kivelson, J. R. Schrieffer, and W. P. Su, Rev. Mod. Phys. **60**, 781 (1988).

[30] J. K. Asbóth, L. Oroszlány, and A. Pályi, *A Short Course on Topological Insulators*, Band Structure and Edge States in One and Two Dimensions, Vol. 919 (Springer, Cham, 2016).

[31] M. Bello, C. E. Creffield, and G. Platero, Sci. Rep. **6**, 1 (2016).

[32] D. Bercioux, M. Governale, V. Cataudella, and V. M. Ramaglia, Phys. Rev. Lett. **93**, 056802 (2004).

[33] M. Hyrkas, V. Apaja, and M. Manninen, Phys. Rev. A **87**, 023614 (2013).

[34] S. D. Huber and E. Altman, Physical Review B **82**, 184502 (2010).

[35] M. Schulze, D. Bercioux, and D. F. Urban, Phys. Rev. B **87**, 024301 (2013).

[36] Y. Nakata, T. Okada, T. Nakanishi, and M. Kitano, Phys. Rev. B **85**, 205128 (2012).

[37] N. Masumoto, N. Y. Kim, T. Byrnes, K. Kusudo, A. Löffler, S. Höfling, A. Forchel, and Y. Yamamoto, New J. Phys. **14**, 065002 (2012).

[38] M. Nixon, E. Ronen, A. A. Friesem, and N. Davidson, Phys. Rev. Lett. **110**, 184102 (2013).

[39] J. Vidal, B. Doucot, R. Mosseri, and P. Butaud, Phys. Rev. Lett. **85**, 3906 (2000).

[40] D. Bercioux, M. Governale, V. Cataudella, and V. M. Ramaglia, Phys. Rev. B **72**, 075305 (2005).

[41] J. Zak, Phys. Rev. Lett. **62**, 2747 (1989).

[42] D. J. Thouless, Phys. Rev. B **27**, 6083 (1983).

[43] D. Meidan, T. Micklitz, and P. W. Brouwer, Phys. Rev. B **84**, 195410 (2011).

[44] R. Jackiw and C. Rebbi, Phys. Rev. D **13**, 3398 (1976).

[45] A. Altland and M. R. Zirnbauer, Phys. Rev B **55**, 1142 (1997).

[46] S. Cheon, T.-H. Kim, S.-H. Lee, and H. W. Yeom, Science **350**, 182 (2015).

[47] E. Alba, X. Fernandez-Gonzalvo, J. Mur-Petit, J. Pachos, and J. Garcia-Ripoll, Phys. Rev. Lett. **107**, 235301 (2011).

[48] D. Abanin, T. Kitagawa, I. Bloch, and E. Demler, Phys. Rev. Lett. **110**, 165304 (2013).

[49] M. Atala, M. Aidelsburger, J. T. Barreiro, D. Abanin, T. Kitagawa, E. Demler, and I. Bloch, Nature Phys. **9**, 795 (2013).

[50] C.-E. Bardyn, S. Huber, and O. Zilberberg, New J. Physics **16**, 123013 (2014).

[51] M. Hafezi, S. Mittal, J. Fan, A. Migdall, and J. Taylor, Nat. Photon. **7**, 1001 (2013).